International Journal of Disaster Risk Reduction 116 (2025) 105133

Contents lists available at ScienceDirect

International Journal of Disaster Risk Reduction

journal homepage: www.elsevier.com/locate/ijdrr

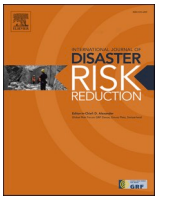

Development of a damage simulator for probabilistic seismic vulnerability assessment of electrical installations

Vahid Hosseinpour [a,*], Ali Saeidi [a], Miroslav Nastev [b], Marie-José Nollet [c]

[a] Department of Applied Sciences, Université du Québec à Chicoutimi, Saguenay, G7H 2B1, Saguenay, QC, Canada
[b] Geological Survey of Canada, Natural Resources Canada, G1K 9A9, Quebec City, QC, Canada
[c] Department of Construction Engineering, École de Technologie Supérieure, H3C1K3, Montreal, QC, Canada

ARTICLE INFO

Keywords:
Seismic vulnerability
Loss estimation software
Hazard analysis
Probabilistic approach

ABSTRACT

Recent earthquakes have revealed the vulnerability of electric power networks to seismic events. To assess their susceptibility to seismic shaking, a user-friendly damage simulator is developed. It consists of two major components: seismic hazard and damage calculation, whereas the inventory of the exposed transmission towers and substations and their vulnerability are provided by the user. The application uses open-source software without any financial costs to users. The computation starts with selection and calculation of either probabilistic or user-defined seismic hazard scenarios including the local site effects. Spectral accelerations at the fundamental vibration period of transmission towers and the peak ground accelerations for substations are considered as intensity measures (IMs) of the transitory seismic shaking. The probabilistic damage assessment incorporates uncertainties in the site parameters and vulnerability of electric installations. The epistemic uncertainty is considered through the logic tree approach introduced in the latest seismic hazard of the National Building Code of Canada, aleatory uncertainty is captured with the Monte Carlo analysis option, whereas the inherent uncertainty related to the structural dynamic response and damage assessment is accounted for with a set of fragility curves describing different damage states. An example of the seismic site characterization, hazard assessment and vulnerability analysis of Hydro-Quebec electrical installations in the Saguenay region, Canada, is presented to illustrate the capacity of the developed software to predict potential damage. Results indicate the resistance of transmission towers and the relatively high vulnerability of substations to seismic shaking.

1. Introduction

The electric power networks (EPN) represent spatially distributed lifeline systems that ensure reliable transmission and supply of electric power to homes and industry [1,2]. They play an important role during and after strong earthquakes minimizing negative impacts, saving lives, and supporting rescue and recovery operations. EPN are complex systems composed of two main components: flexible transmission towers, which support conductive cables and insulators, and relatively rigid transformation substations with their own set of components. Their structural types vary according to the line voltage and the environment in which they are built [3–5]. The tower structural system can be either lattice steel (e.g. waist-type, double circuit, guyed-V and guyed cross-rope) or tubular.

* Corresponding author.
E-mail address: vahid.hosseinpour1@uqac.ca (V. Hosseinpour).

https://doi.org/10.1016/j.ijdrr.2024.105133
Received 11 November 2023; Received in revised form 19 December 2024; Accepted 19 December 2024
Available online 20 December 2024

Substations consist of transformers, circuit breakers, switchgear and associated control devices [6].

High-voltage EPN have been proven susceptible to heavy dynamic loads generated by geohazards (seismic shaking and ground failures) and atmospheric hazards (accumulation of ice and winds). Their seismic vulnerability has been highlighted during past strong earthquakes [7–10]. EPN are particularly vulnerable due to their significant spatial extent and since they contain a variety of vulnerable components often not designed to withstand lateral loads [11,12]. The preferred approach for preventing earthquake negative effects relies on incorporating the latest design principles for new EPN, however, most of existing transmission lines were generally built with minimal consideration of the seismic effects [13]. Assessing the potential seismic risk of existing EPN represents therefore the first phase in preparation of management and mitigation plans.

Due to the importance of EPN in everyday life, a number of studies have been devoted to the assessment of their seismic vulnerability [14]. It can be assessed empirically observing occurred physical damage following strong earthquakes, or applying experimental and analytical methods focused on the vulnerability of individual components [12]. Other studies, on the other hand, focused on the seismic performance and operation of the EPN systems as a whole, considering substations as nodes, where most of the vulnerable pieces of equipment are concentrated, and transmission lines as links with comparatively lower seismic vulnerability [15].

To determine the seismic performance of EPN for a variety of seismic scenarios, Shinozuka et al. applied a simple neural network analysis with a two-state assumptions, failure or safe [16]. Buritica et al. used complex system theory to analyse interacting EPN elements and model probability of seismic failure scenarios applying fragility curves integrating probability of failure as function of the seismic shaking intensity [17]. Likewise, a flow-based analysis model for evaluating the substation's earthquake-resistance capability is presented with performance indicators and directed graph logic system analysis [18]. A rapid seismic risk assessment framework was also introduced replacing traditional time-consuming Monte Carlo (MC) simulations with an improved minimum cut set algorithm, where minimal cut set represent a group of components whose failure generate failure of the entire system [19]. A probabilistic resilience assessment framework for ultra-high-voltage converter stations is presented, using a matrix-based approach to determine the functional state between network nodes [20]. As well, probabilistic models for post-disaster recovery of EPNs were developed using the Bayesian approach, highlighting the need for additional data collection and suggesting future research directions [21].

In parallel, significant effort has been made on the development of seismic risk assessment software for prediction of overall earthquake impacts [22], such as Hazard US (HAZUS) [23] and its different versions (e.g. Ergo [24]), Haz-Taiwan [25], SELENA [26], HazCan [27], InaSAFE [28], CAPRA [29], DBELA [30], OpenQuake [31] and the ER2 web application [32]. Some countries have created their own customised software, whereas international projects, such as the Global Earthquake Model (GEM), are developing tools that can be used worldwide [22,33]. These tools generally calculate the probability of physical damage and the corresponding economic and social losses. They are based on the systematic acquisition and interpretation of the following parameters: (i) seismic hazard, (ii) inventory of exposed buildings and infrastructures, and (iii) their corresponding vulnerabilities [34,35]. Current software packages, however, do not adequately address specific challenges posed by the EPN seismic vulnerability.

The objective of this study is to develop a user-friendly damage simulator for evaluation of the seismic vulnerability of major EPN components power transmission towers and substations. The simulator consists of two major modules (i) site parameters (e.g., shear wave velocity in the top 30 m): and seismic hazard analysis which consists of probabilistic and user defined what-if event scenarios, including local site effects; and (ii) damage assessment to determine the probability of exceedance of different damage states of the electrical installations given the seismic hazard scenario. The damage assessment incorporates uncertainties in the site parameters, uncertainty considered through the logic tree approach introduced in the latest seismic hazard of Canada, whereas the inherent

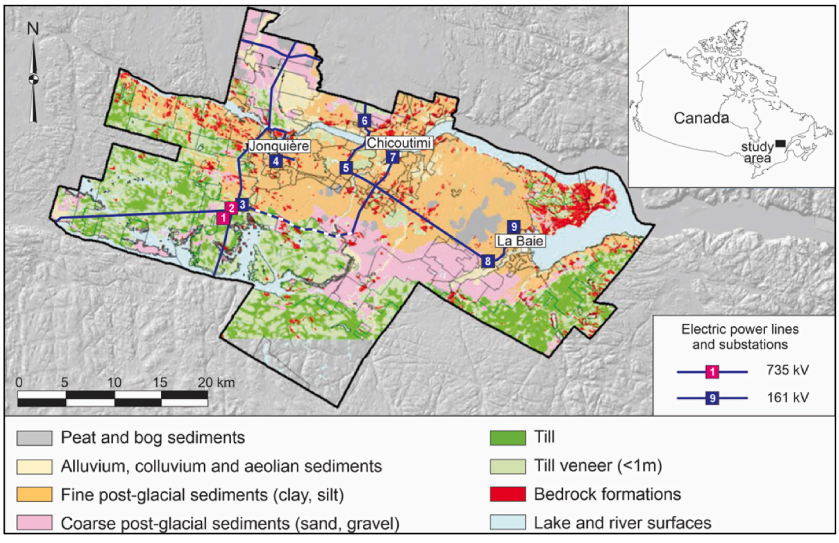

Fig. 1. Study area of the Saguenay region with the spatial distribution of electrical installations and surficial geology map as background ([6,36]). The dashed blue-white line is considered in this study to test the damage module of electrical towers.

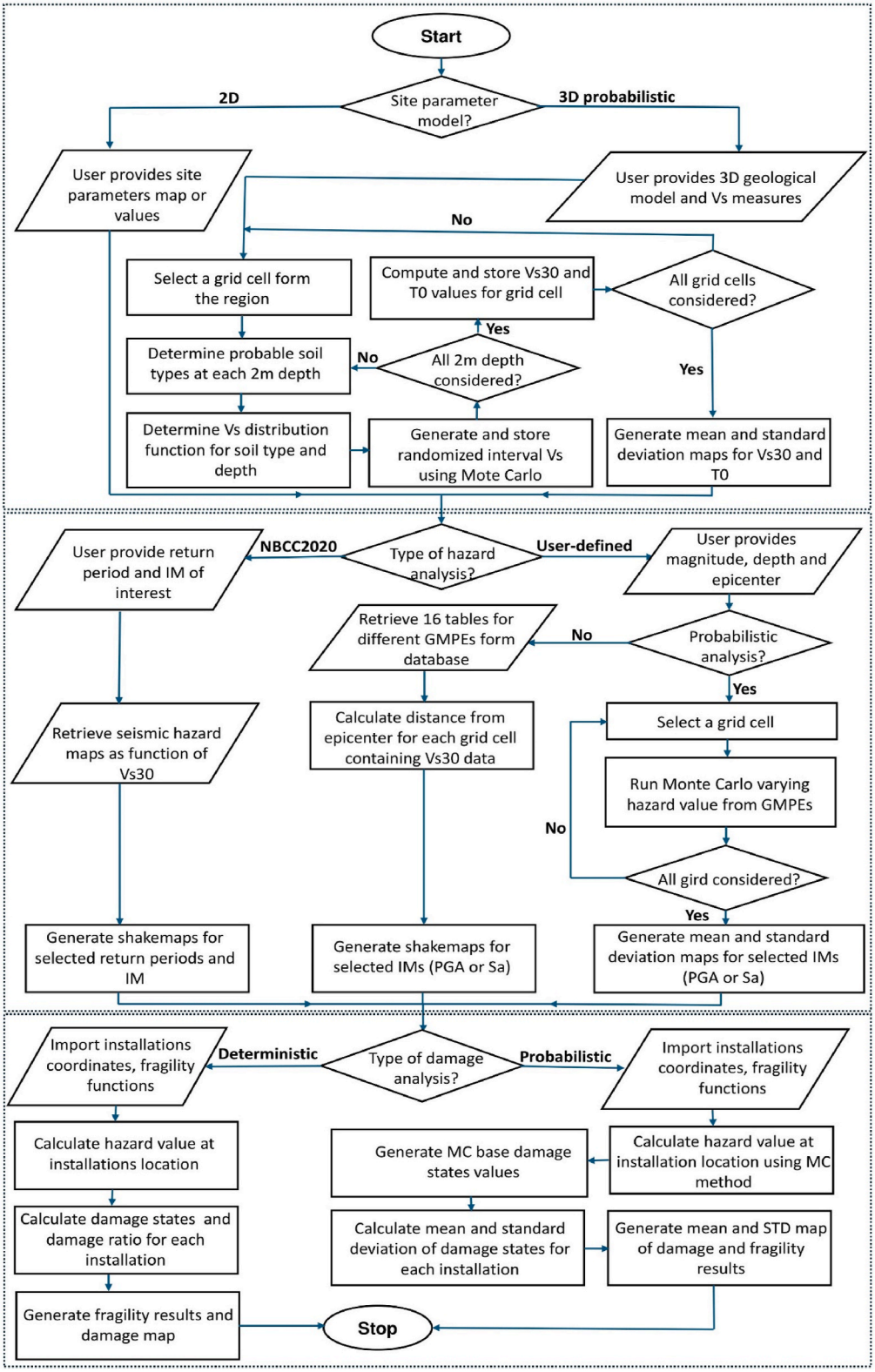

Fig. 2. General workflow of the damage simulator.

uncertainty related to the structural dynamic response is accounted for with a set of fragility curves describing different damage states. The City of Saguenay in eastern Canada was selected as a study area characterized with the presence of a high-voltage transmission lines, moderate seismic activity and heterogeneous surficial sediments which may considerably amplify the earthquake transitory motion (Fig. 1).

2. Programming workflow

The development of an efficient simulator of seismic damage to EPN installations relies on a series of interdependent tasks and variables: choice of programming language, including method and architecture; determination of the seismic hazard at bedrock level; determination of site effects; inventory of assets at risk; and selection of respective vulnerability functions [34]. Following the decision on software architecture, the choice of programming language was the first step in the development of software for seismic risk estimation. The Python programming language was selected for this application based on its versatility and suitability for complex scientific calculations. Python has a large and still growing community of developers and users and provides abundance of resources and support for users. It also has a rich library of modules and scientific packages, (e.g., NumPy, SciPy and Matplotlib), facilitating the implementation of various algorithms and models. Furthermore, Python is an open-source code, freely available and can be modified to meet specific needs [37]. The use of Python in this application contributes to rapidly generate accurate and reliable results and facilitates the continued development and improvement of the software over time. In addition, its high-level interface makes it easy to interact with other software, improving the efficiency of the workflow. The general workflow of the damage simulator components is presented in Fig. 2.

As indicated in Fig. 2, upon the program's initiation, it guides users to choose from two primary modules: site parameters and/or hazard analysis, and damage calculation. For seismic hazard assessment, the user has the option to provide their own local site parameters maps, or to use the embedded Monte Carlo (MC) base probabilistic approach. The user can then select among the 2020 National Building Code of Canada (NBCC2020) probabilistic seismic hazard, for a return period of 2475 years or the user defined what-if scenario. In the latter case, the user has to provide the basic earthquake parameters, e.g., magnitude (M), coordinates of the epicenter (x, y) and depth. The damage simulation is then run for the embedded or for user provided electrical installations (type and coordinates) and respective vulnerability curves. The different damage states in which a given electrical installation will be following the earthquake are calculated in a probabilistic manner for the IM computed at that location. Details on each of the above steps are given in the following sections.

3. Seismic hazard module

The seismic hazard in this study is described in terms of spatial distribution of the intensity of the transitory seismic shaking at bedrock level. Other induced seismic hazards such as permanent ground deformations caused by liquefaction, landslide, lateral spread, etc., are not considered. The potential amplification of the bedrock motion due to local geological and geotechnical conditions is based on the evaluation of the time averaged shear wave velocity in the top 30 m, Vs_{30}. The next most common parameters, the fundamental vibration period of the soil column T_o Ref. [38], is also calculated, although for the time being it is not used in the hazard computations. The standard intensity measures (IMs) of the seismic shaking are peak ground acceleration (PGA) and spectral acceleration for selected vibration periods of interest (S_a).

3.1. Probabilistic seismic hazard scenarios

A probabilistic seismic hazard represents the likelihood of a given ground shaking intensity to occur at a specific location over a given time period. It is obtained as a weighted average of the impacts of all potential seismic sources that affect a location, each defined with its own fault or fault area, magnitude–frequency relationship and respective ground motion prediction equation (GMPE) which accounts for the source-to-site attenuation of the seismic waves. The shaking intensity is typically determined for reference conditions of seismic bedrock with average shear wave velocity of $V_s = 3000$ m/s, or for the interface between engineering bedrock and surficial sediments defined with $V_s = 760$ m/s [39].

The probabilistic seismic hazard embedded in the damage simulator corresponds to the NBCC2020 6th generation seismic hazard model for stable crustal conditions in eastern Canada. The model uses a multiple logic tree approach and is based on a 50/50 weighting strategy between the three GMPEs AA13 [40] and 13 GMPEs known as NGA-East-13 [40,41]. The retained design return period in this study is 2475 years, which corresponds to the exceedance probability of 2 % in 50 years. The shaking intensity at the ground surface is calculated incorporating the local site conditions through the embedded Vs_{30} map for the Saguenay region, or for user provided CSV file with comma-separated Vs_{30} values and coordinates for the study area of interest. The probabilistic values of the considered IMs, PGA and Sa at the ground surface are obtained applying respective amplification factors suggested in NBCC2020 [40]. The log-normal distribution was assumed for the Vs_{30} mean and standard deviation map generation process [42,43]. The other option is to consider a probabilistic site parameter model discussed in detail in section 3.3.

3.2. User defined what-if scenario

The evaluation of the user defined seismic scenarios hazard is based on a point source approximation of the fault or the seismic zone of interest. The seismic source is defined based on user provided earthquake parameters (M, x, y, depth) and combined with GMPEs

corresponding to the seismic settings of the region. In this case, the considered earthquake magnitude should still correspond to the magnitude–frequency relationship of the seismic source and determined over a realistic return period, thus involving the notion of likelihood. The epicentral distances (D) to the studied location of the electrical installation, or the grid cells into which the entire study area is divided, is then automatically calculated. The source-to-site attenuation is then computed with the 16 GMPEs from the 6th generation Canadian seismic hazard model [44,45]. In addition, the damage simulator applies MC simulation to account for aleatory uncertainties in the seismic IMs (PGA and S_a). MC simulations are conducted using the SciPy library, specifically leveraging various distribution types from SciPy.stats to generate IMs as random variables [37]. The mean and standard deviation values for PGA, Sa, and other intensity measures (IMs) are provided in terms of log(IM) according to NBCC 2020 [46]. Typically, hazard parameters are simulated using a log-normal distribution [39,41]. However, in this study, we simulated the IMs using a normal distribution. Subsequently, we exponentiated the log(IM) results to obtain the IM values and their standard deviations in the form of a log-normal distribution.

The generated random IMs are stored in the form of a Pandas Dataframe for efficient manipulation and computation. The subsequent calculations are performed using NumPy functions, benefitting from their speed and efficiency in numerical computations. This approach ensures a robust and efficient workflow for the MC simulations, providing a solid foundation for the study's results.

Upon the generation of probabilistic seismic hazard map at bedrock level, the shaking intensity at the ground surface is calculated incorporating the local site conditions through the embedded Vs_{30} map for the Saguenay region, or for user provided Vs_{30} CSV file for the study area of interest (Fig. 2). The user has also the option to consider the probabilistic Vs_{30} model (Fig. 2).

3.3. Uncertainties in site parameters

Beside deterministic Vs_{30} maps, both the probabilistic seismic hazard and the user defined options allow for incorporation of uncertainties in Vs_{30}, which further propagate into the seismic IMs at the ground surface. To this end, a MC approach was applied for the Saguenay region considering: (i) probabilistic 3D geological model represented with the probability of occurrence of surficial sediments, their thickness and depth, and (ii) probabilistic assessment of the site parameters Vs_{30} and T_0 based on the shear wave velocity Vs-depth probability distributions.

The existing probabilistic 3D geological model for the Saguenay study area consisting of 75 × 75 × 2 m block elements was used to demonstrate this capacity [47]. For each 2m depth, the best fit V_s probability distribution function was determined based on the field V_s measurements for the encountered soil type in the (from below): glacial deposits, fine clayey sediments and coarse sandy soils [48,49]. In this study, the Vs database of postglacial sediments was compiled from field measurements at 16 locations [50]. SCPT tests were

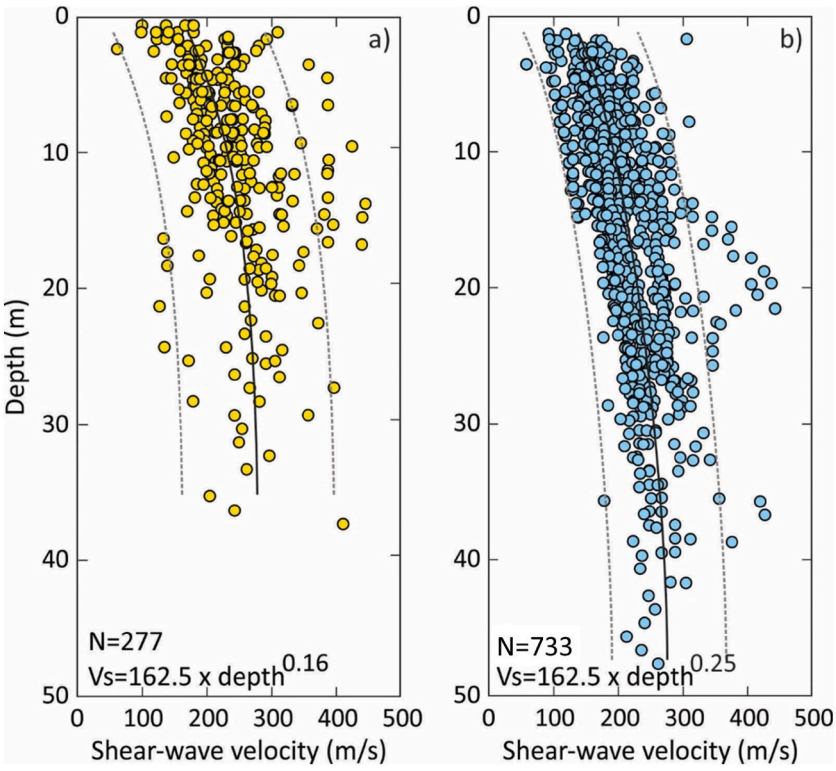

Fig. 3. Vs data for: a) coarse sediments (sand and gravel), b) fine sediments (clay and silt). Bold black lines illustrate conventional regression functions; dashed red lines show 95 % confidence intervals.

conducted within the study area by the authors with a complete set of measurements. In total, there are 733 Vs observations in fine sediments and 277 in coarse sediments. The Vs-depth data are given in Fig. 3 together with regression analysis [51,52]. The coarser sandy unit display slightly higher Vs than finer clayey unit with important overlapping and apparent discrepancies well within the observed variabilities. Both soil units exhibit a large amount of scatter in their Vs data due to the heterogeneity in the grain-size distribution and overburden pressure compaction.

Ten most common distribution functions were considered: normal, lognormal, beta, gamma, Pearson, inverse Gaussian, exponential, Weibull, triangular and the uniform distribution function. They were stored for each grid cell in a temporary database and MC simulations were performed to assess the vertical and spatial variabilities of V_s, Vs_{30} and T_0 to accounting for uncertainties. For each grid cell the vertical stratigraphy was first simulated sampling the most probable soil type at each 2 m depth. The corresponding best-fit V_s probability distribution function was retrieved for that soil type and depth, and a V_s value was randomly generated. The number of sampled V_s values was determined according to the thickness of the geological units in the stratigraphic column. The Vs_{30} value was computed as the average travel time for the top 15 block elements, whereas T_0 was obtained for the whole soil column through the quarter-wavelength equation [53]. In a single run, the same procedure was repeated for all grid cells of the study area. The MC simulations were run until the stability of the V_s values were reached. To determine the stop condition, i.e. the maximum number of simulations, four example grid cells were selected based on the geological profiles encountered in the top 30 m: #1 contains glacial and post-glacial sediments in the top 30 m, #2 and #3 include post-glacial sediments, whereas #4 includes all the geological units. Fig. 4 shows the convergence of the predicted average Vs_{30} with the number of MC simulations.

As is apparent from Fig. 4, the stability of the response variable Vs_{30} is attained already after a few hundred simulations regardless of the stratigraphy. This is an important observation since a potential relationship between the number of simulations and the stratigraphy could introduce an unwanted bias or an unnecessary increase of the CPU time. It was therefore decided to limit the number of simulations of the seismic site parameters to 1000 as a more conservative option. In each MC simulation, the above process was repeated for each of the 155,800 grid cells. Following each MC simulation, the Vs_{30} and T_0 realizations are stored in the database. At the end of the 1000 simulations, the standard deviations maps are created as quantitative measures of the considered uncertainties.

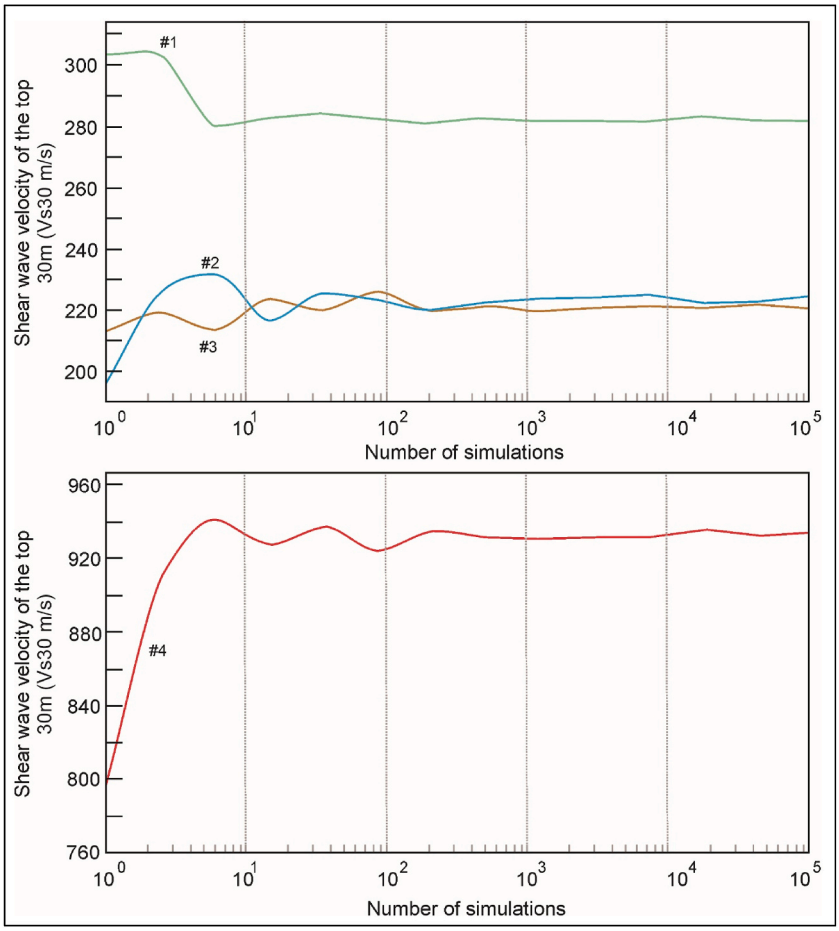

Fig. 4. Convergence of the mean Vs30 with the increasing number of realizations.

4. Vulnerability analysis

The vulnerability analysis consists in: (i) inventory of the electrical installations (transmission towers and substations) exposed to the seismic hazard scenarios, (ii) selection of representative fragility functions, and (iii) damage calculation [34]. Fragility functions correlate the probability of exceeding thresholds for different damage states ranging from no to complete damage with a given level of shaking intensity. They are defined as a lognormal function of damage with mean value at 50 % damage and a standard deviation generally in the order of 0.7–0.8. The fragility functions are intended mainly for use in urban and regional risk assessments and are representative for a group of structures with similar dynamic response characteristics. They can be generated based on field observations of damage, analytical studies, expert judgment or a combination of these approaches, and the chosen method depends on the type, frequency and quality of available data, expertise, resources, and the size of the study area.

4.1. Transmission towers

Although a number of studies have focused on fragility functions for most common structures (e.g. buildings and bridges), there is currently no standardized taxonomy available for the seismic vulnerability of electrical installations. A comprehensive literature review was conducted to select appropriate vulnerability functions representative for the existing Hydro-Quebec transmission towers. The power transmission line to the Saguenay region extends over more than 1000 km from James Bay, where electricity is produced in eight hydroelectric power plants. To reduce potential losses of the initial energy, the voltage in this line is increased to 735 kV, which is equivalent to four standard 315 kV lines. The voltage increase is accompanied with increased diameter of the conductor cables bundled in series of two to four. To support the high-voltage conductors, three types of transmission towers are used [54]: (i) waist-type tower is the most commonly used transmission tower suitable for power-lines crossing rough terrain and carrying voltages between 110 kV and 735 kV; (ii) guyed-V tower is a V-shaped lattice tower that is supported and secured by stay wires that carry voltages between 230 kV and 735 kV; and (iii) double circuit tower is designed for smaller footprints with height range of 25 m–60 m, and capacity to carry voltages of up to 315 kV (Fig. 5).

To describe the structural damage condition effectively, three damage states (performance levels) with three respective thresholds

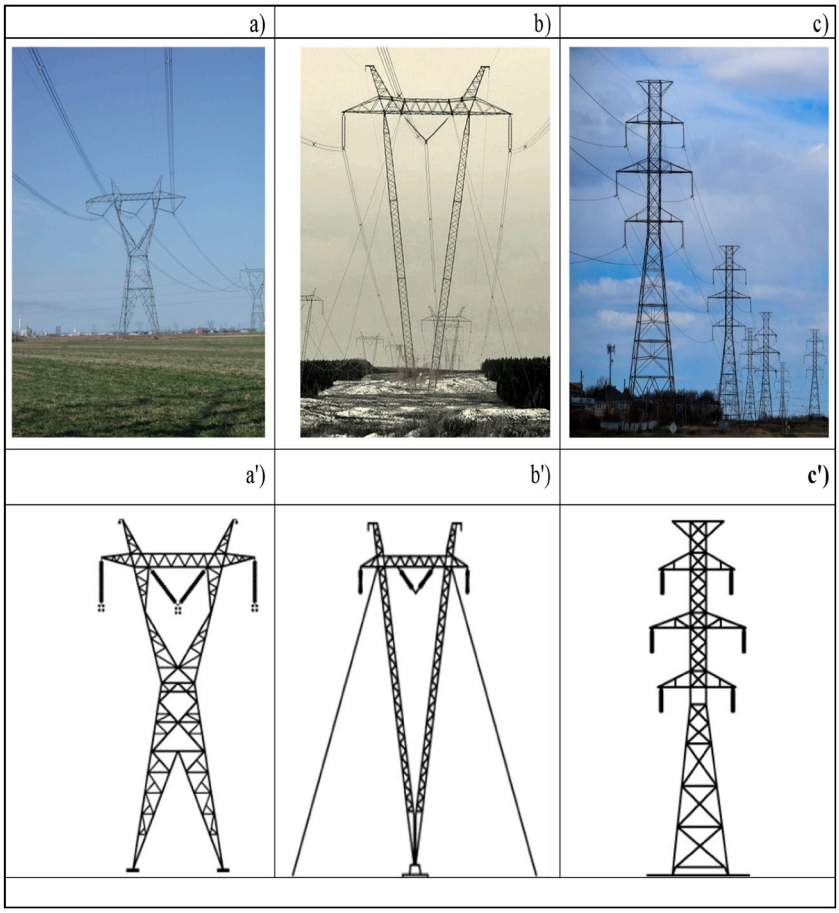

Fig. 5. Hydro-Quebec transmission towers: a-a') Waist-type, b-b') Guyed-V and c-c') Classic double-circuit power transmission towers [6].

were defined using the pushover analysis [55]. In the serviceability state (SA), the tower remains in the elastic domain during an earthquake and continues to operate with minimal or no repair after the earthquake. In the damage control state (DC), the tower sustains considerable damage and plastic deformation, which depending on the extent of damage may be beyond economical repair. In the collapse prevention state (CP), the tower sustains damage, such that it can no longer support the weight of the conductors and its own weight [13]. The maximum intersegment drift ratio (ISDR), defined as the ratio between the differential lateral displacement between two consecutive segments of a tower and their respective height, was assumed as the response parameter that correlates best with tower damage. Similar to the seismic fragility of steel moment frames, the ISDR threshold values for the three damage states were 0.8 %, 2 % and 4 % of the height between consecutive segments [13]. The spectral acceleration (S_a) at the predominant period of vibration of the tower (T) was considered as an IM applied to convert the pushover curve into a fragility function. The fragility curves for the classic double-circuit power transmission towers in the Saguenay study area are shown in Fig. 6.

The fragility curves in Fig. 6 represent the probability that the transmission tower will reach or exceed the predefined limit states (damage thresholds) as a function of the spectral acceleration at 1s. Considering the absence of established loss functions for vulnerability assessment in transmission towers, we have defined the following damage levels as follows: $D_0 = 0$, indicating no damage, and $D_3 = 3$, representing complete damage or collapse. The calculation of the final damage ratio for each tower is performed using the following equation,

$$Dm = \sum P_{DS_i} \times D_i \tag{1}$$

where, Dm is the mean damage ratio to the towers, P_{DS_i} denotes the probability of each damage state and D_i corresponds to the damage value associated with each respective damage state. Note that the damage simulator allows users to introduce their own vulnerability functions for damage calculation.

4.2. Substations

Electrical substations make part of standard electric power transmission and distribution systems that transform voltage from high to low. The major components of a substation include transformers, circuit breakers and switchgear to isolate different parts of the electric power systems, capacitors to smooth the voltage flow, and other control devices [6]. Transformer steel structures are the largest pieces of equipment in a substation, capable of holding several cubic meters of mineral oil used as an insulating material. If not properly designed and anchored, this type of equipment can be particularly vulnerable to seismic shaking. Due to its direct relation to inertial forces, the peak ground acceleration PGA represents a common measure of the seismic shaking intensity in stiff structures, such as substations. These types of rigid structures basically reproduce the seismic shaking of the ground surface. Therefore, the damage potential of substations was defined in terms of PGA. The fragility curves for North American substation types developed for the HAZUS software are used herein [56]. They define five damage states which can be attained during a strong seismic shaking: none, slight, moderate, extensive, and complete, for low, medium and high voltage and anchored or unanchored substations. In Fig. 7 are given the fragility functions for unanchored high and low voltage substations.

Since the substations contain many different components, the damage states shown in Fig. 7 actually determine the percentage of subcomponents that suffered damage: 0 % (none), 5 % (slight), 40 % (moderate), 70 % (extensive) and 100 % (complete damage).

4.3. Damage computation

The damage calculation workflows within the software are composed of multiple individual calculators. Currently, the developed software has two distinct damage calculation workflows (Fig. 2). The first workflow is designed to calculate damage resulting from a single user-defined seismic event for which shakemaps of IMs (PGA and Sa1.0s in this case) are generated.

The second workflow is more complex and designed to compute damage considering the uncertainty associated with both site parameters and hazard parameters. First, the MC approach is applied to account for uncertainties in site parameters. Another set of MC

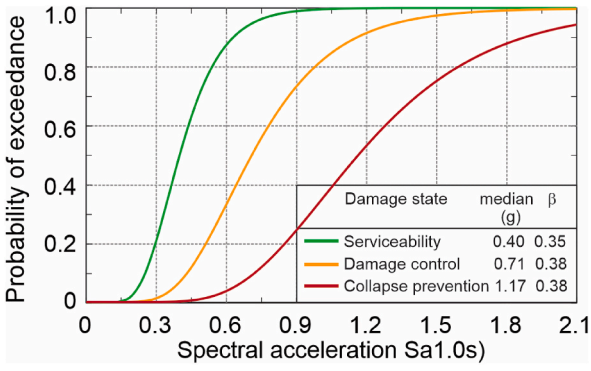

Fig. 6. Fragility curves for a 87.3 m high Classic Double-circuit tower (Modified from Ref. [35]).

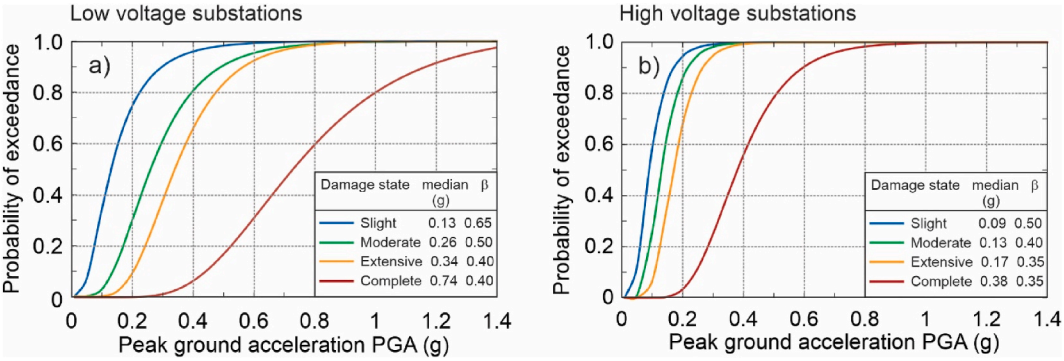

Fig. 7. Fragility curves for high and low voltage substations with standard components [49].

simulations is conducted to account for uncertainties in the hazard parameters (PGA or S_a 1.0), applying the normal distribution and standard deviation defined for the GMPEs [39,57]. The results are then used to calculate the mean and standard deviation of damage states.

5. Results

The final results are generated in three different steps: (i) site parameters (Vs_{30} and T_0), (ii) seismic hazard at ground surface (PGA or S_a 1.0), and (iii) damage estimates to transmission towers and substations. For the first two steps analyses may be conducted as deterministic or probabilistic with MC based multiple scenarios, whereas, due to the probabilistic nature of the fragility functions, the damage assessment generates the likelihood of being in a given damage state. To demonstrate the software's capabilities, an example is given herein for the Saguenay region, eastern Canada. The study region of approximately 880 km^2 was modelled with a grid of 155,800 2D 75 × 75 m raster cells and 1,061,200 3D 75 × 75 × 2 m-thick block elements extending from the ground surface to the bedrock interface. An existing 3D geological model was used providing the extent, thickness and depth of each of the considered soil types (till, clay, sand and gravel). A total of 733 Vs-depth observations in fine sediments and 277 in coarse sediments were used for the consecutive statistical modelling. Detailed results are presented in the following subsections.

5.1. Site parameters (V_{S30} and T_0) and associated uncertainties

The deterministic results of the site parameters Vs_{30} and T_0 are given in Fig. 8, whereas Fig. 9 shows the respective probabilistic maps of mean and standard deviation values obtained with the MC approach. MC simulations were used to sample the probability of occurrence of each soil units in each 2m thick block element, and respective V_s values were sampled from the best-fit distribution function for each block element. Both figures display high-resolution maps of Vs_{30} and T_0 and identify regions that are more susceptible to seismic amplification.

As illustrated in Fig. 8, areas covered by thick sediments exhibit lower Vs_{30} values and higher T_0 values. In contrast, points characterized by till or rock outcrops demonstrate an increase in Vs_{30} values and a decrease in T_0 values.

The mean Vs_{30} and T0 maps are accompanied with the uncertainty expressed by the spatial distribution of the standard deviation of

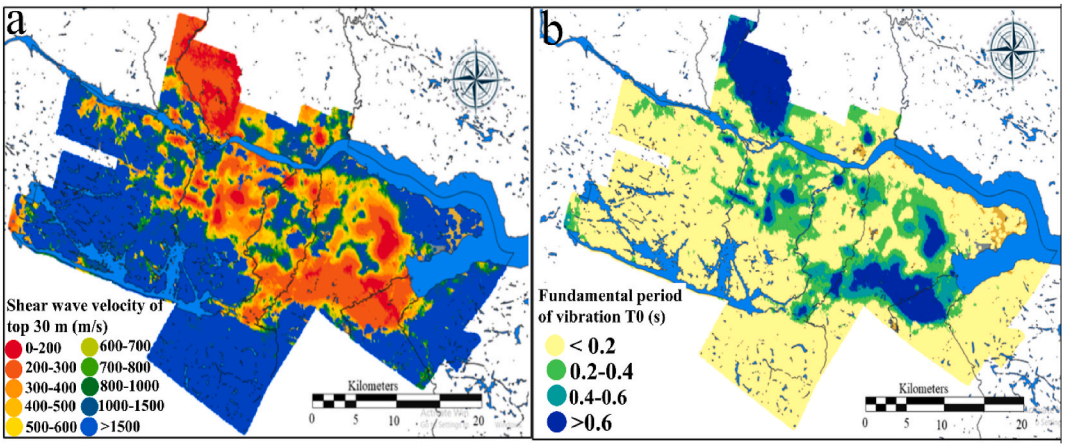

Fig. 8. Deterministic site parameters maps: a) Vs_{30} b) T_0.

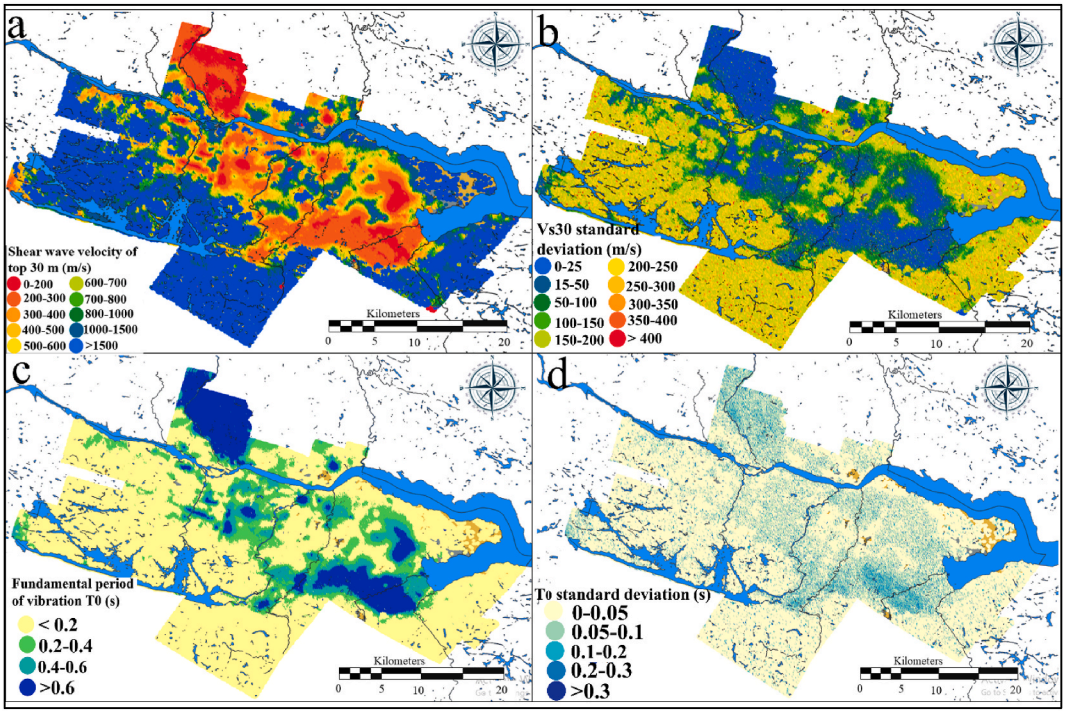

Fig. 9. Probabilistic site parameters maps using the 3D probabilistic Vs model and MC simulations: a) *Vs_{30}, b) Standard deviations of Vs_{30}, c) Mean T_0 and d) T_0 standard deviations.*

site parameters (see Fig. 9-b and Fig. 9-d). The site parameters spatial distribution follows approximately the discrepancy patterns of the surficial geological units are shown in Fig. 1. By comparing the surficial geology map (Fig. 1) and the standard deviation map, lower uncertainty is observed in grid-cells with higher sediment thickness. On the contrary, higher uncertainty is observed in grid cells with shallow sediment thickness, mainly till deposits overlying bedrock. Rapid transitions from relatively low (Vs_{30} <200 m/s) to high Vs_{30} at rock outcrops (Vs_{30} >2500 m/s) can be seen between neighbouring cells, as well.

Upon comparing the deterministic site parameters map with the maps derived from the MC based approach, significant differences in parameter values can be observed in certain areas. These areas are characterized mainly with moderate to high soil thickness.

To evaluate the efficiency of the proposed method and conduct the validation of the proposed site characterization model, the 1000 MC realizations of Vs_{30} and T_0 were corroborated with the respective deterministic maps. To emphasise the dissimilarities between the Vs_{30} maps in Figs. 8 and 9, a ratio is computed as the difference between the deterministic and probabilistic Vs_{30} values normalized to the standard deviation σ_{Vs30}. Similarly, in the case of the fundamental period, the ratio is computed as the difference between the deterministic and probabilistic T_0 values normalized to the standard deviation σ_{T0}. The comparison between the two approaches is presented in Fig. 10.

Fig. 10 highlights areas where the differences between the two approaches are comparatively the higher, i.e., a ratio >1 indicates differences which exceed the standard deviation (highlighted in red for Vs_{30} and purple for T_0).

5.2. Seismic hazard assessment with integration of uncertainty

The PGA and Sa results obtained from the hazard analysis can be categorised into (i) user-defined event scenarios, (ii) probabilistic hazard scenarios, and (iii) seismic hazard based on MC scenarios.

5.2.1. User-defined event scenarios

To demonstrate this type of earthquake scenarios, a magnitude 5.9 earthquake with a depth of 10 km was considered. The PGA and *Sa* 1.0 results are presented in Fig. 11. The software also allows users to select other IMs, e.g., spectral accelerations, for consecutive damage assessment.

5.2.2. Probabilistic hazard scenarios

In Fig. 12 is given the spatial distribution of the *Sa* 1.0 values at the ground surface, with a probability of exceedance of 2 % over 50 years.

As depicted in Fig. 12, the PGA values across the Saguenay region range from 0.5 to 0.6 g, aligning with the hazard values specified in NBCC 2020. However, the variation for *Sa*1.0 appears higher than that of PGA, ranging between 0.2 and 0.4. Furthermore, the Sa1.0

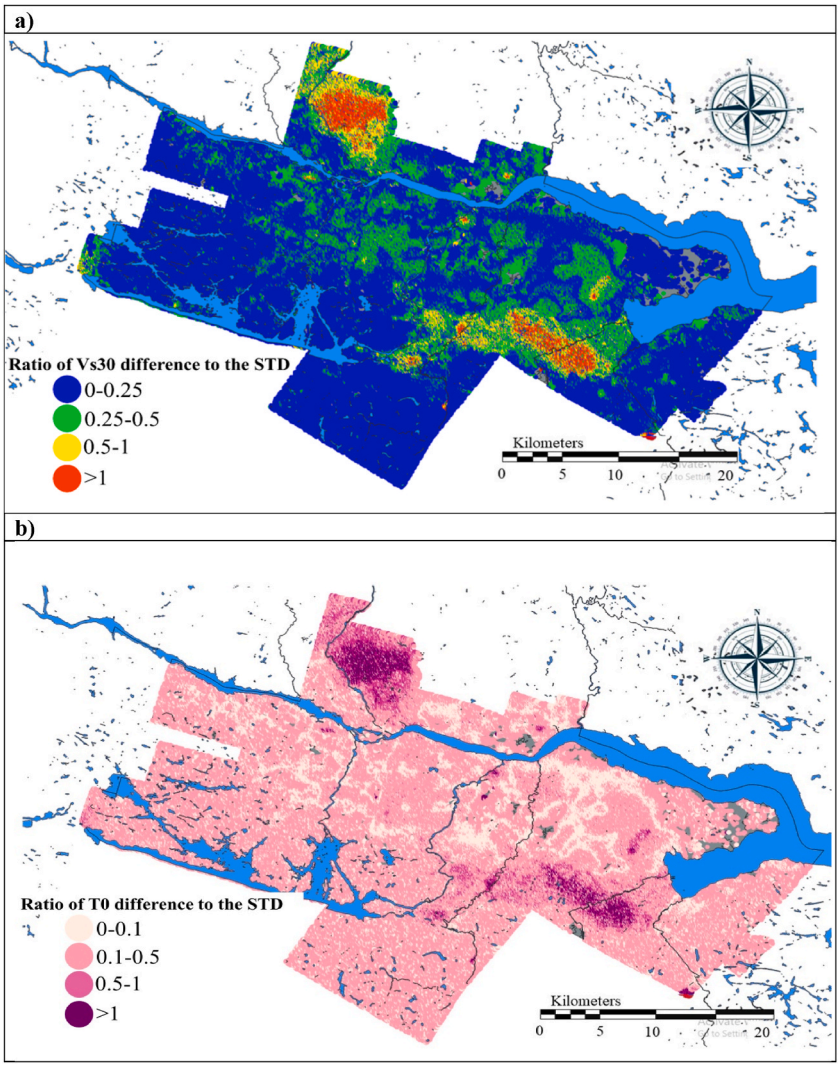

Fig. 10. Spatial distribution of the differences between the deterministic and MC based probabilistic method a) Vs30 values normalized to σ_{Vs30}, and b) T_0 values normalized to σ_{T0}.

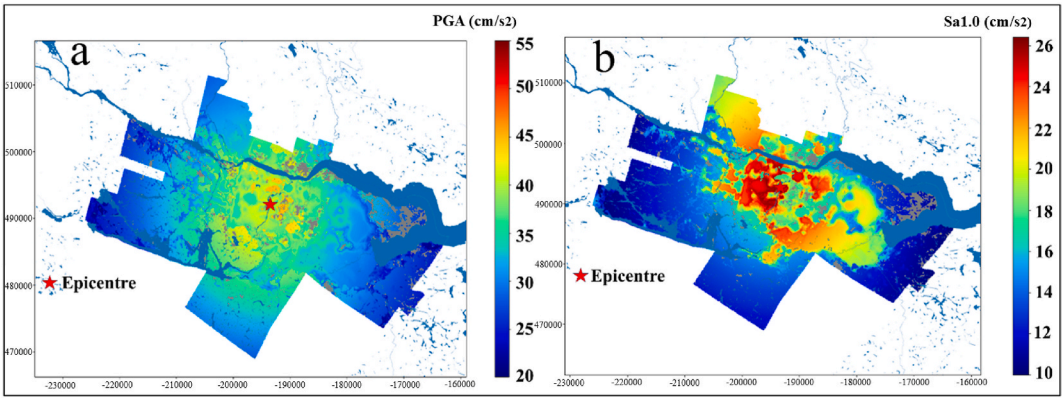

Fig. 11. User defined scenario hazard maps for an earthquake with M5.9 and depth of 10 km.

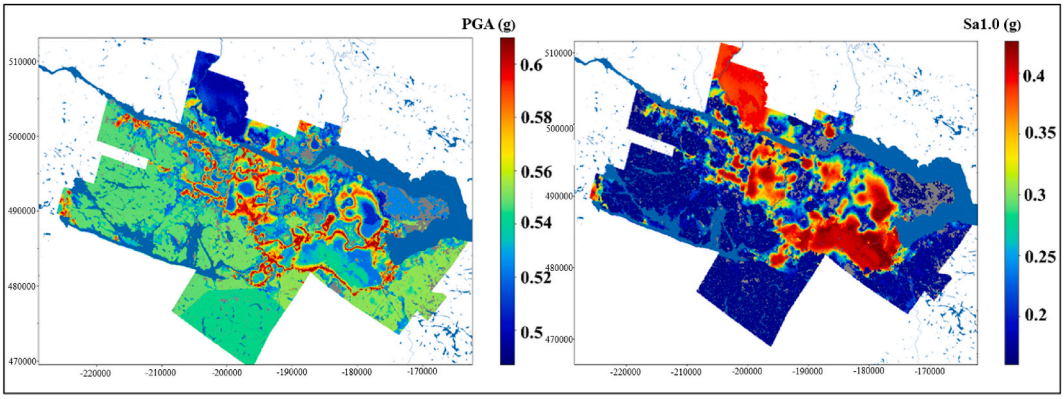

Fig. 12. Probabilistic hazard maps with probability of exceedance of 2 % in 50 years for the Saguenay region, a) PGA, b) Sa1.0.

map indicates higher hazard values in areas with thicker sediments, suggesting the influence of soil thickness on the Sa values.

5.2.3. Probabilistic hazard scenario with uncertainty in Vs30 and GMPEs

As described in the methodology section, one of the novelties of the developed software is systematic tracking of uncertainties in both site parameters, V_{S30} and T0, and the applied GMPEs. To this end MC method is implemented to generate the respective hazard scenarios. Geological uncertainties were simulated first applying the probabilistic 3D geological model followed by the application of a MC method to assess Vs uncertainty. The uncertainty in the GMPEs was considered based on MC method running 1000 realizations for each grid cell to assess the Vs means and standard deviations. These realizations represent the input for the damage assessment module. Fig. 13a and c display the spatial distribution of the mean PGA and *Sa* 1.0 values, whereas the respective standard deviations are shown in Fig. 13b and d.

As illustrated in Fig. 13, the shaking intensity decreases at points away from the earthquake's epicenter. A comparison of Fig. 13-a and 13-c with Fig. 1 indicates that regions with larger sediment thickness exhibit higher PGA and Sa1.0 values, as opposed to areas with rock outcrops or covered with till veneer which show relatively lower shaking intensities. Similarly, the respective standard

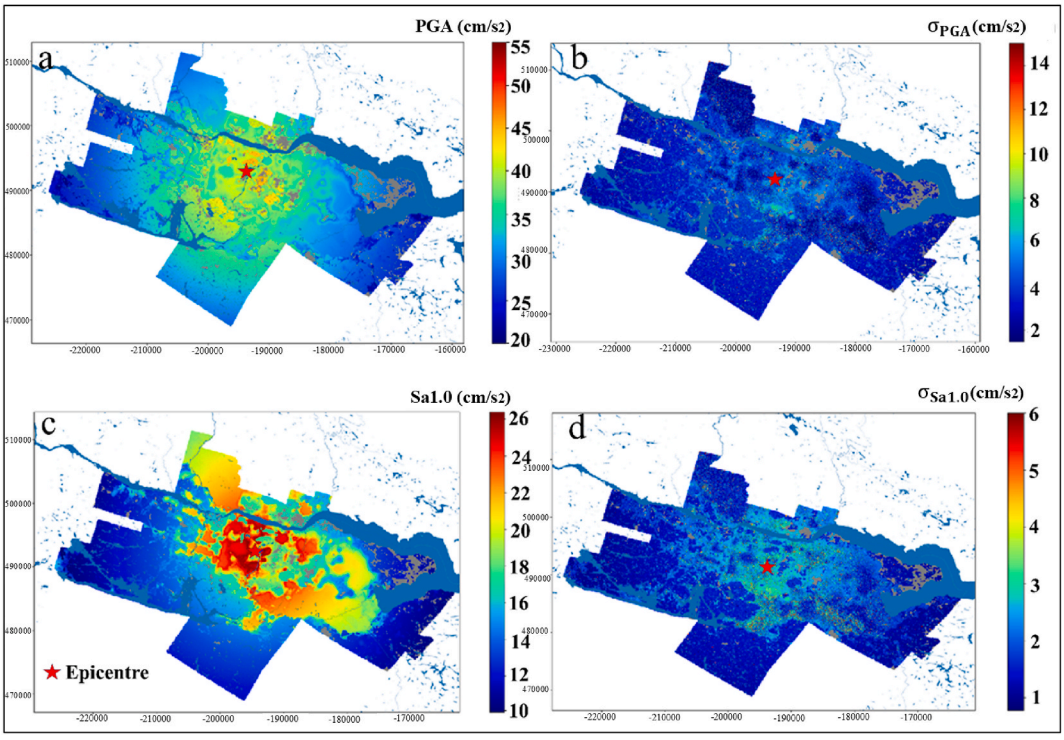

Fig. 13. User defined scenario including uncertainties in Vs30 and GMPEs: a-b) mean PGA and standard deviation and c-d) mean Sa1.0 and standard deviation.

deviations also higher in the same regions characterized with thicker sediments, Fig. 13-b and Fig. 13-d.

5.3. Damage outputs

The third set of results is related to damage assessment of the considered electrical installations. Users have the choice of evaluating damage a single tower and/or substation, or for a power-line segment with multiple towers and substations. As mentioned above, the computation of the input seismic shaking corresponds to one of the three seismic scenarios: deterministic, MC-based probabilistic and NBCC2020 probabilistic scenarios.

5.3.1. Damage assessment for deterministic hazard scenarios

To evaluate the potential impacts of a user-defined scenario, damage assessment was conducted for the replica of the 1988 Saguenay earthquake scenario with a magnitude of 5.9 and a depth of 28 km. The results for individual electrical installations are given in Fig. 14 and computed for two example towers, #T15 and #T42, and high voltage substation #1 and low voltage substation #1.

As expected, the results indicate higher damage susceptibility of the electrical substations than that of the transmission towers. The same conclusion could have been made by simply comparing the respective fragility curves. Whereas the towers remain predominantly undamaged or only slightly damaged, the considered substations show moderate to severe damage, highlighting their high seismic vulnerability. This analysis underscores the need for further investigation into improving the earthquake resilience of substations.

Next, a damage assessment was performed along the Hydro-Quebec transmission lines in the Saguenay region. This assessment involved consideration of 95 electric towers and 6 substations, each with respective coordinates. The damage map is depicted in Fig. 15. High voltage substations and low voltage substations are shown respectively with horizontal rectangles and vertical rectangles on the map.

As expected, Fig. 15 indicates that the majority of the towers are unaffected by the M5.9 seismic scenario. The substations, on the other hand suffered relatively high impacts. The two high-voltage substations along the transmission line sustained significant damage, while only low to moderate damage occurred to low-voltage substations at various locations in Saguenay. The observed damage levels correspond with post-earthquake observations following the Saguenay earthquake, during which the transmission towers remained

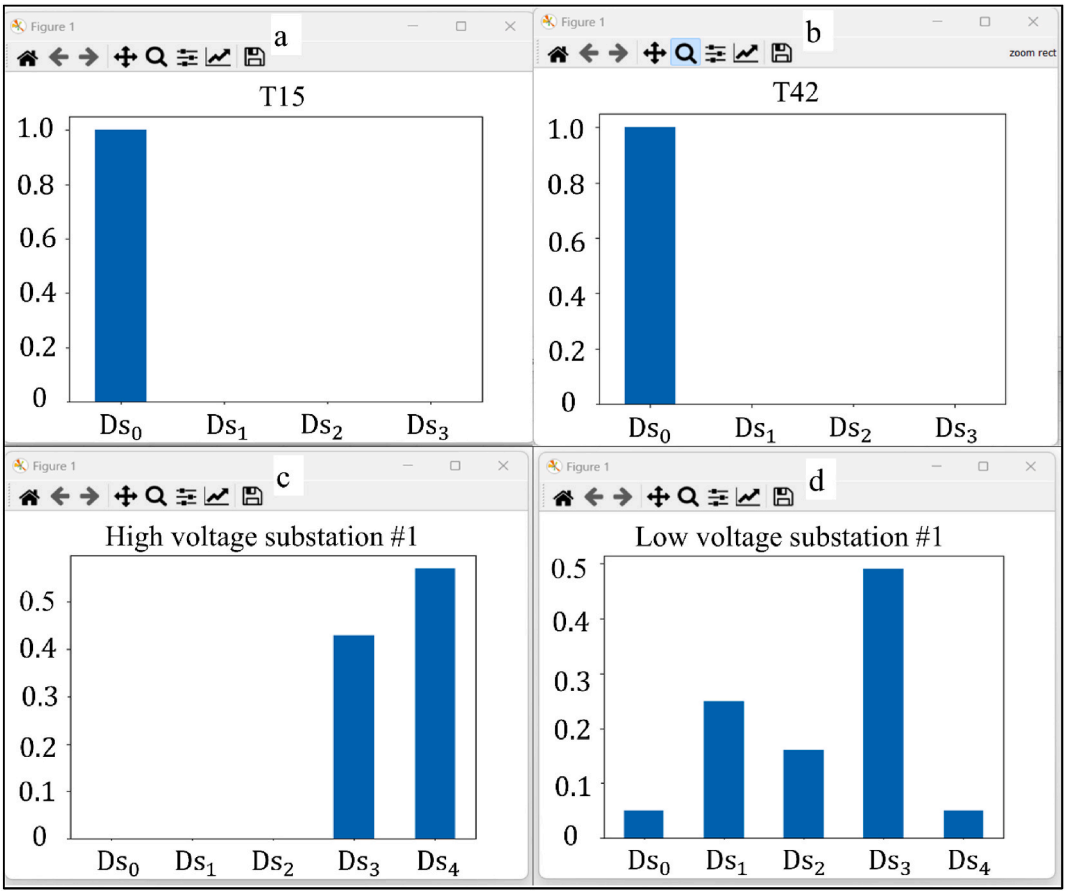

Fig. 14. Predicted damage for the Saguenay 1988 earthquake scenario: a-b) towers #T15 and #T42, and c-d) high voltage and low voltage substation.

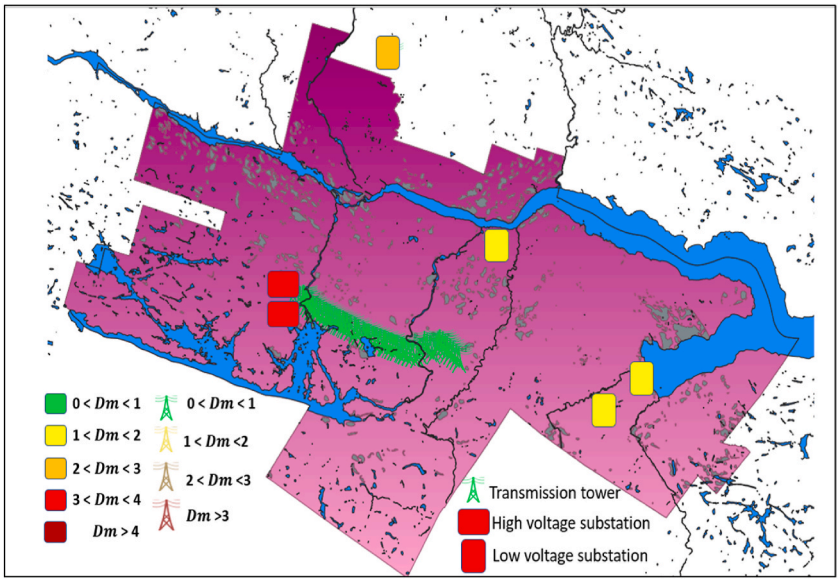

Fig. 15. Damage assessment for the Hydro-Quebec installations in Saguenay for earthquake scenario with M5.9 and depth 28 km.

unaffected, yet certain substations experienced considerable damage.

5.3.2. Damage results based on MC method

The capacity of the developed damage simulator's to track uncertainties in damage evaluation was evaluated through the implementation of a probabilistic damage analysis using the MC approach. This method facilitates the generation of multiple damage realizations, each associated with different probabilities of occurrence, thus enabling the capture of the variability in the site parameters (V_s and T_0) and in the shaking intensity (PGA and $Sa1.0$). Such an approach provides a comprehensive understanding of the potential range and likelihood of damage under varying conditions. The results of the MC analysis for two example towers and substations are presented in Fig. 16.

Fig. 17 presents the results of the MC damage assessments for towers and substations in the Saguenay region exposed to the M5.9 and depth 28 km event, along with the associated uncertainties.

In this analysis, it was observed again that the majority of the towers remained undamaged, while the substations, particularly the high-voltage ones, incurred substantial damage. Fig. 17-b illustrates the standard deviation of the damage, represented by colored triangles. This depiction indicates that the standard deviation of damage is notably higher for substations compared to transmission towers.

5.3.3. NBCC2020 probabilistic scenario for return period of 2475 years

A probabilistic seismic hazard scenario based on NBCC2020 for 2 % probability of exceedance in 50 years was considered for this type of damage analyses. As was the case in the previous simulations, electrical installations of the Hydro-Quebec power-line segment in the Saguenay region were considered. The respective damage results are presented in Fig. 18.

As depicted in Fig. 18, under the given hazard scenario, the majority of the exposed towers appear to be largely unaffected. In contrast, the exposed substations exhibit a significantly higher susceptibility to seismic hazard, suggesting a potential for damage during probabilistic seismic hazard scenarios. It can also be observed that some low-voltage substations experienced higher damage compared to those analyzed using MC based damage analysis method with user defined earthquake scenario. This observation may suggest that the consideration of NBCC 2020probabilistic hazard values provides a more conservative approach for analysis of the potential damage.

6. Conclusion

This study describes the development process of a damage simulator for assessing the seismic vulnerability of electric transmission towers and substations. The simulator was developed to address the need for a user-friendly tool for evaluation of seismic risk to electrical installations, transmission towers and substations, at a so called "push of the button" approach. To achieve this objective, the damage simulator enables site parameter analysis (V_s and T_0), assessment of the hazard intensity measures (PGA and Sa) and damage calculation (fragility and damage factors). Each module of the simulator employs two types of analyses, i.e. deterministic and probabilistic, thus providing a variety of choices to the end user.

One of the novelties of the developed software is in the incorporation of an algorithm for systematic tracking of geological and geotechnical uncertainties incorporated in the site parameters (Vs_{30}, T_0) and applied GMPEs. The geological and geotechnical un-

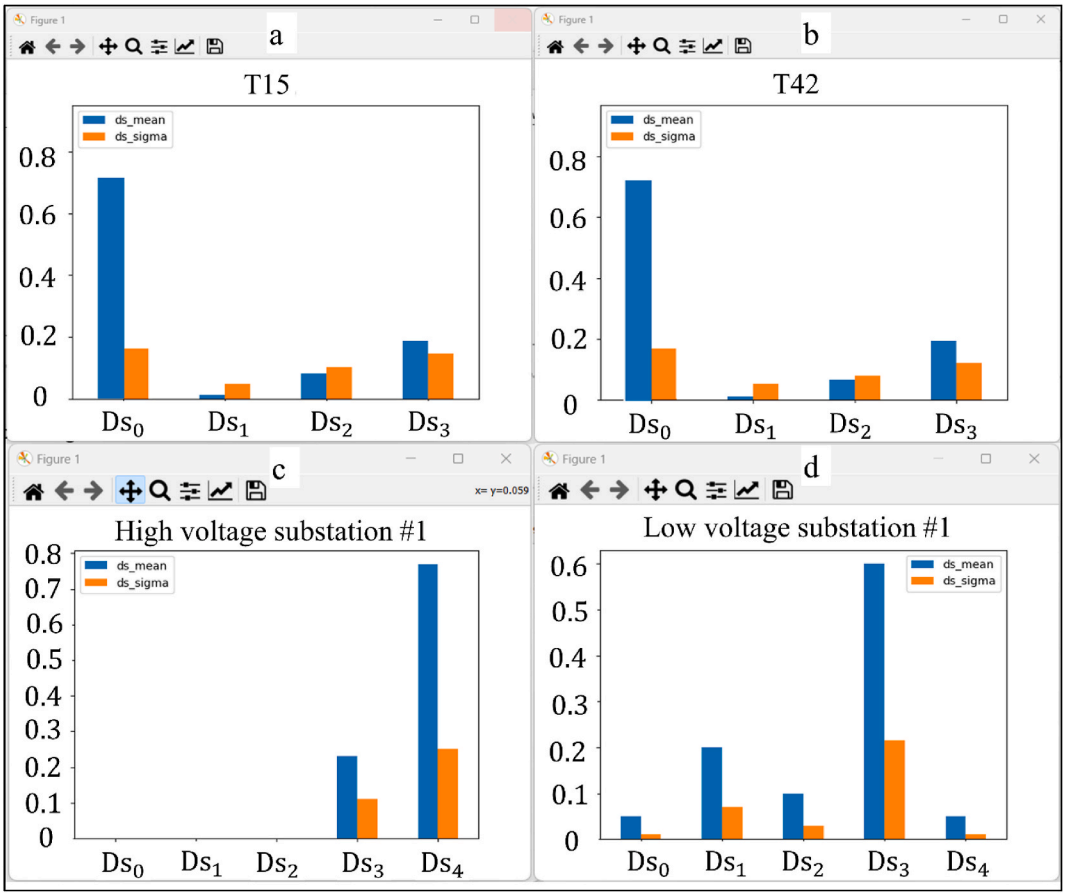

Fig. 16. MC base fragility analysis for transmission towers #T15 and #T42, and high and low voltage substations.

certainties were assessed applying a 3D probabilistic geological block model, whereas V_s-depth MC-based simulations were conducted to assess the uncertainties in V_s, V_{S30} and T0. This approach accounts for the precise probability distribution of Vs with depth, taking into consideration the impacts of specific sedimentation and erosion processes that occurred in the study region.

To provide a better user experience, the most advanced Python libraries are applied to perform thousands of MC calculations in a matter of a few minutes only. To assess the hazard parameters (PGA and Sa1.0), the software is capable of generation of user-defined scenario, MC multi-scenario probabilistic analyses and conventional probabilistic scenario for a given return period. Epistemic uncertainty is captured using multiple (13) GMPE models that were recently introduced in NBCC2020. The aleatory uncertainty is addressed through the MC- based algorithm.

One key advantage of using the MC method in the hazard assessment is the ability to model a range of potential scenarios, each with varying combinations of input parameters. This multi-scenario approach can provide a more comprehensive assessment of hazard risks, enabling users to understand the range of possible outcomes better and prepare accordingly. By incorporating the variability and uncertainty of site parameters and hazard intensities, the MC method produces a broader range of potential outcomes than a traditional deterministic or probabilistic analysis. Furthermore, the ability to generate multiple realizations enables users to assess the likelihood of estimated damage. By providing a more detailed and probabilistic understanding of potential damage, such approach offers users with valuable information for consecutive risk management efforts.

The damage assessment process employs the concept of vulnerability expressed through sets of fragility curves that provide the probability of reaching or exceeding different damage states given the intensity of the seismic shaking. Two IMs at the location of the electrical installation were considered in the analyses: PGA for relatively rigid substation components and Sa1.0 for the flexible transmission towers. Users have the choice to evaluate damage for a single electrical installation (tower and/or substation), or for a complete power-line segment with multiple towers and substations.

In order to assess the software's performance, a comprehensive case study was carried out for transmission towers and substations operated by Hydro-Quebec in the Saguenay region, eastern Canada. The results indicate the capabilities of the damage simulator to evaluate the seismic damage to electrical installations, but also highlight the increased vulnerability of substations, while the transmission towers remain mainly unaffected by the seismic shaking. Due to its versatility, the damage simulator can be used for various engineering applications, including probabilistic site characterization, seismic hazard assessment, and damage calculation, all of which are important for effective seismic risk management. While the current version of the software is primarily designed for

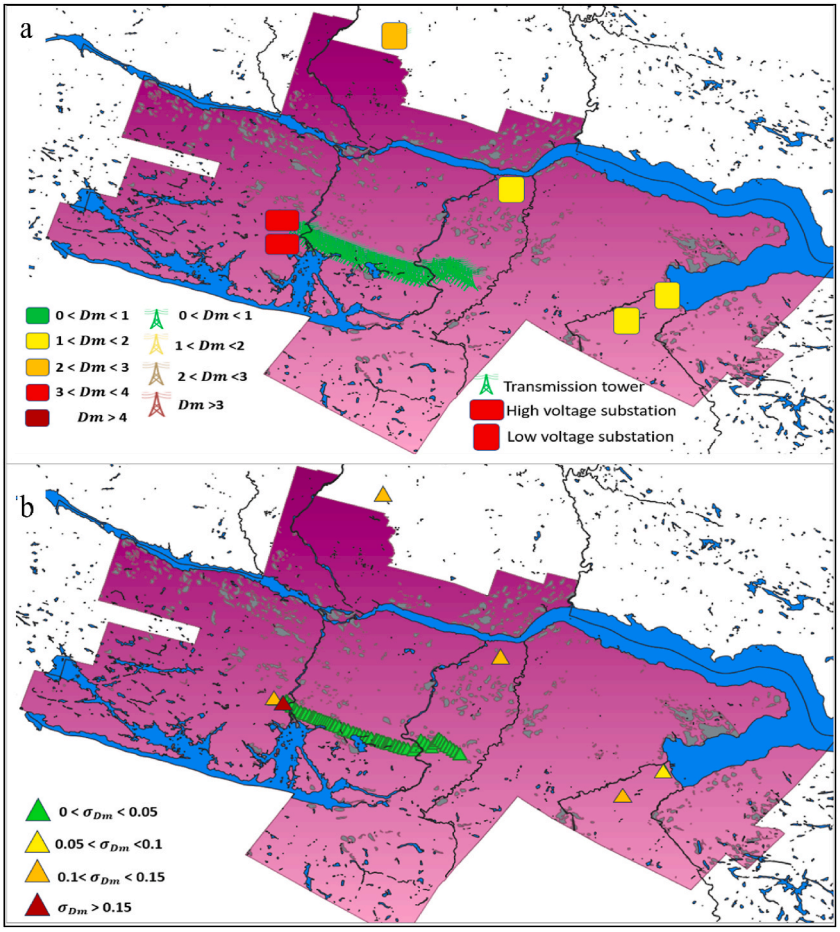

Fig. 17. Probabilistic MC-based damage assessment for the Hydro-Quebec installations in Saguenay for a scenario with M = 5.9 and depth 28 km, a) mean damage b) standard deviation of damage.

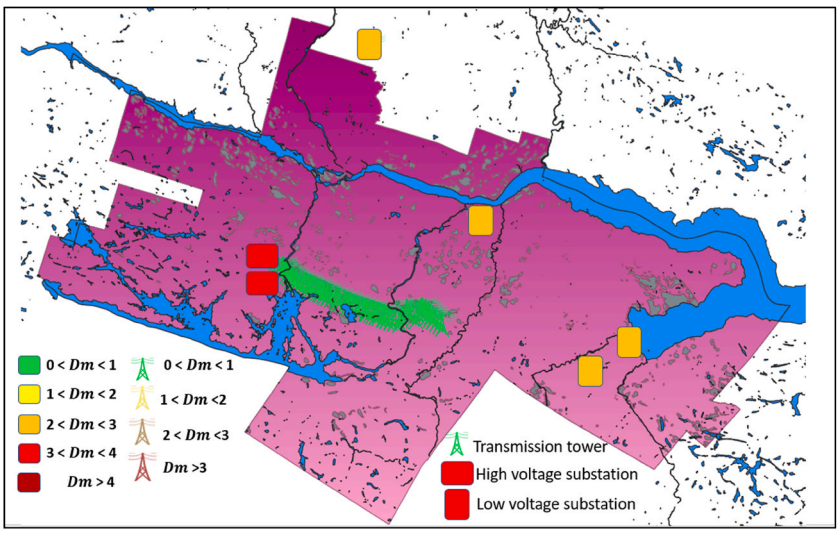

Fig. 18. Damage calculation based on probabilistic scenario of 2 % probability of exceedance in 50 years.

assessing the seismic vulnerability of transmission towers and substations under Canadian seismic settings, its open-source nature allows for broader applications, such as for risk assessment of different types of infrastructures (building, bridges, etc.) in different geographical regions worldwide.

CRediT authorship contribution statement

Vahid Hosseinpour: Writing – original draft, Visualization, Validation, Software, Methodology, Investigation, Formal analysis, Data curation, Conceptualization. **Ali Saeidi:** Writing – review & editing, Supervision, Resources, Project administration, Methodology, Funding acquisition, Conceptualization. **Miroslav Nastev:** Writing – review & editing, Supervision, Conceptualization. **Marie-José Nollet:** Writing – review & editing, Supervision, Funding acquisition, Conceptualization.

Funding

This research was partially funded by the Natural Sciences and Engineering Research Council of Canada (NSERC) and Hydro-Quebec under project funding no. RDCPJ 521771-17 and also CRC-NSERC 950–232724.

Declaration of competing interest

The authors declare that they have no known competing financial interests or personal relationships that could have appeared to influence the work reported in this paper.

Acknowledgements

The authors would like to thank the members of the CERM-PACES project for their cooperation to conduct the field tests and provide access to the database.

Data availability

Data will be made available on request.

References

[1] K. Pitilakis, H. Crowley, A.M. Kaynia, SYNER-G: Typology Definition and Fragility Functions for Physical Elements at Seismic Risk: Buildings, Lifelines, Transportation Networks and Critical Facilities, Springer Science & Business Media, 2014.
[2] F. Pavel, R. Vacareanu, C. Arion, A. Aldea, A. Scupin, Seismic risk assessment of lifelines in Bucharest, Int. J. Disaster Risk Reduc. 66 (2021) 102629, https://doi.org/10.1016/j.ijdrr.2021.102629.
[3] T. Ghazal, E. Elkassas, M.I. El-Masry, Conductive cables vibrations effect on lattice steel transmission towers, J. Steel Struct. Construct. 5 (151) (2019) 7.
[4] C. Hashimoto, M. Numada, T. Kodama, S. Taniguchi, T. Aoki, Y. Seki, Securing electric power sources for modern disaster risk reduction in Japan, Int. J. Disaster Risk Reduc. 95 (2023) 103871, https://doi.org/10.1016/j.ijdrr.2023.103871.
[5] X. Liu, Q. Xie, Resilience-based post-earthquake recovery strategies for substation systems, Int. J. Disaster Risk Reduc. 96 (2023) 104000, https://doi.org/10.1016/j.ijdrr.2023.104000.
[6] H. Quebec, Power transmission | towers | hydro-québec. http://www.hydroquebec.com/learning/transport/types-pylones.html, 2023.
[7] M. Reyners, Lessons from the destructive Mw 6.3 Christchurch, New Zealand, earthquake, Seismol Res. Lett. 82 (3) (2011) 371–372.
[8] M. Naddaf, Turkey-Syria earthquake: what scientists know, Nature (2023).
[9] J.M. Eidinger, Gujarat (Kutch), India, M7. 7 earthquake of January 26, 2001, and Napa M5. 2 Earthquake of September 3, 2000, ASCE Publications, 2001.
[10] A.K. Tang, I. zmit (Kocaeli), Turkey, earthquake of August 17, 1999 including Duzce earthquake of November 12, 1999: lifeline performance, ASCE Publications, 2000.
[11] A.J. Schiff, Guide to Improved Earthquake Performance of Electric Power Systems, National Institute of Standards and Technology, Building and Fire Research, 1998.
[12] X. Liu, Q. Xie, A multi-strategy framework to evaluate seismic resilience improvement of substations, Reliab. Eng. Syst. Saf. 245 (2024) 110045, https://doi.org/10.1016/j.ress.2024.110045.
[13] L. Tian, X. Gai, B. Qu, Shake table tests of steel towers supporting extremely long-span electricity transmission lines under spatially correlated ground motions, Eng. Struct. 132 (2017) 791–807.
[14] K. Pitilakis, T. Xenos, K. Kakderi, M. Alexoudi, G. Theofilogiannakos, Seismic risk analysis of electric power transmission systems. Proceedings and Monographs in Engineering, Water and Earth Sciences, 2007, pp. 583–584.
[15] R. Giannini, A. Vanzi, Seismic reliability of electric networks and interaction with other damage indicators. Proc. 12th World Conference on Earthquake Engineering, 2000.
[16] M. Shinozuka, S. Chang, T. Cheng, Advances in seismic performance evaluation of power networks, in: APEC Seminar on Earthquake Disaster Management of Energy Supply Systems, 2003.
[17] J. Buritica, S. Tesfamariam, M. Sánchez-Silva, Seismic vulnerability assessment of power transmission networks using complex-systems based methodologies, 15th World Conf. Earthq. Eng (2012) 24–28.
[18] H. Liang, Q. Xie, System vulnerability analysis simulation model for substation subjected to earthquakes, IEEE Trans. Power Deliv. 37 (4) (2022) 2684–2692, https://doi.org/10.1109/TPWRD.2021.3114279.
[19] X. Liu, Q. Xie, W. Zhu, Rapid assessment of substation earthquake risk based on minimal cut sets, Elec. Power Syst. Res. 229 (2024) 110175, https://doi.org/10.1016/j.epsr.2024.110175.
[20] X. Liu, Q. Xie, A multi-model probabilistic framework to evaluate seismic resilience of UHV converter stations, Eng. Struct. 300 (2024) 117153, https://doi.org/10.1016/j.engstruct.2023.117153.
[21] Y. Handa, E. Opabola, C. Galasso, A Bayesian approach for estimating the post-earthquake recovery trajectories of electric power systems in Japan, Sustain. Resil. Infrastruct. 1-14. https://doi.org/10.1080/23789689.2024.2303801.

[22] V. Hosseinpour, A. Saeidi, M.-J. Nollet, M. Nastev, A comprehensive review of seismic hazard and loss estimation software. GeoCalgary 2022 (The 75th Canadian Geotechnical Conference), Calgary, Alberta, Canada, 2022.
[23] C.A. Kircher, R.V. Whitman, W.T. Holmes, HAZUS earthquake loss estimation methods, Nat. Hazards Rev. 7 (2) (2006) 45–59.
[24] M.-A.E. Mae Center, MAEviz Software, Urbana, IL: MAE Center, University of Illinois at Urbana-Champaign, 2006.
[25] C.-H. Yeh, C.-H. Loh, K.-C. Tsai, Overview of Taiwan earthquake loss estimation system, Nat. Hazards 37 (1–2) (2006) 23–37, https://doi.org/10.1007/s11069-005-4654-z.
[26] S. Molina, C. Lindholm, A logic tree extension of the capacity spectrum method developed to estimate seismic risk in Oslo, Norway, J. Earthq. Eng. 9 (6) (2005) 877–897.
[27] M. Ulmi, C.L. Wagner, M. Wojtarowicz, J.L. Bancroft, Hazus-MH 2.1 Canada, user and technical manual: earthquake module, Nat. Res. Canada (2014).
[28] A.I.F.D.R. Aifdr, Australia-Indonesia facility for disaster reduction, InaSafe-Eartquake tool, Available Online at: http://inasafe.org/, 2020. (Accessed 20 May 2020).
[29] E. Reinoso, M. Ordaz, O. Cardona, G. Bernal, M. Contreras, AFTER 10 YEARS OF CAPRA, 2018.
[30] H. Crowley, R. Pinho, J. Bommer, J. Bird, Development of a displacement-based method for earthquake loss assessment, European school for advanced studies in reduction of seismic risk, Pavia, Research Report No. ROSE-2006 1 (2006).
[31] V. Silva, H. Crowley, M. Pagani, D. Monelli, R. Pinho, Development of the OpenQuake engine, the Global Earthquake Model's open-source software for seismic risk assessment, Nat. Hazards 72 (3) (2014) 1409–1427.
[32] A. Abo El Ezz, A. Smirnoff, M. Nastev, M.-J. Nollet, H. McGrath, ER2-Earthquake: interactive web-application for urban seismic risk assessment, Int. J. Disaster Risk Reduc. 34 (2019) 326–336, https://doi.org/10.1016/j.ijdrr.2018.12.022.
[33] V. Silva, H. Crowley, R. Pinho, H. Varum, Development of an Open-Source Platform for Calculating Losses from Earthquakes, University of Aveiro, Portugal, 2014.
[34] V. Hosseinpour, A. Saeidi, M.-J. Nollet, M. Nastev, Seismic loss estimation software: a comprehensive review of risk assessment steps, software development and limitations, Eng. Struct. 232 (2021) 111866, https://doi.org/10.1016/j.engstruct.2021.111866.
[35] R.V. Whitman, T. Anagnos, C.A. Kircher, H.J. Lagorio, R.S. Lawson, P. Schneider, Development of a national earthquake loss estimation methodology, Earthq. Spectra 13 (4) (1997) 643–661.
[36] R.-A. Daigneault, P. Cousineau, E. Leduc, G. Beaudoin, S. Millette, N. Horth, G. Allard, Rapport Final sur les Travaux de Cartographie des Formations Superficielles Réalisés dans le Territoire Municipalisé du Saguenay-Lac-Saint-Jean, Ministère des Ressources naturelles et de la Faune du Québec, Quebec City, QC, Canada, 2011.
[37] P. Virtanen, R. Gommers, T.E. Oliphant, M. Haberland, T. Reddy, D. Cournapeau, E. Burovski, P. Peterson, W. Weckesser, J. Bright, SciPy 1.0: fundamental algorithms for scientific computing in Python, Nat. Methods 17 (3) (2020) 261–272, https://doi.org/10.1038/s41592-019-0686-2.
[38] R.D. Borcherdt, Effects of local geology on ground motion near San Francisco Bay, Bull. Seismol. Soc. Am. 60 (1) (1970) 29–61, https://doi.org/10.1785/BSSA0600010029.
[39] G.M. Atkinson, J. Adams, Ground motion prediction equations for application to the 2015 Canadian national seismic hazard maps, Can. J. Civ. Eng. 40 (10) (2013) 988–998, https://doi.org/10.1139/cjce-2012-0544.
[40] M. Kolaj, T. Allen, R. Mayfield, J. Adams, S. Halchuk, Ground-motion models for the 6th generation seismic hazard model of Canada. 12th Canadian Conference on Earthquake Engineering, 2019.
[41] C.A. Goulet, Y. Bozorgnia, N.A. Abrahamson, N. Kuehn, L. Al Atik, R.R. Youngs, R.W. Graves, G.M. Atkinson, Central and Eastern North America Ground-Motion Characterization (NGA-East), Univ. of California, Berkeley, CA (United States), 2018.
[42] B. Hassani, G.M. Atkinson, Site-effects model for central and eastern North America based on peak frequency and average shear-wave VelocitySite-effects model for CENA based on peak frequency and average shear-wave velocity, Bull. Seismol. Soc. Am. 108 (1) (2018) 338–350.
[43] M. Nastev, M. Parent, N. Benoit, M. Ross, D. Howlett, Regional VS30 model for the St. Lawrence lowlands, eastern Canada, Georisk 10 (3) (2016) 200–212. https://10.1080/17499518.2016.1149869.
[44] Canadian Commission on Building and Fire Codes, National Building Code of Canada: 2020, National Research Council of Canada, 2022.
[45] J. Adams, T. Allen, S. Halchuk, M. Kolaj, Canada's 6th generation seismic hazard model, as prepared for the 2020 national building code of Canada. 12th Can. Conf, Earthquake Engineering, 2019.
[46] M. Kolaj, S. Halchuk, J. Adams, Sixth-generation seismic hazard model of Canada: final input files used to generate the 2020 National Building Code of Canada seismic hazard values, Nat. Res. Canada (2023).
[47] M. Salsabili, A. Saeidi, A. Rouleau, M. Nastev, 3D probabilistic modelling and uncertainty analysis of glacial and post-glacial deposits of the city of Saguenay, Canada, Geosciences 11 (5) (2021) 204.
[48] V. Hosseinpour, A. Saeidi, M. Nastev, M.-J. Nollet, A Monte-Carlo based Vs30 microzonation map for Saguenay, QC. 8th Canadian Conference on Geotechnique and Natural Hazards, Canadian Geotechnical Society, Quebec City, Canada, 2022, p. 689.
[49] V. Hosseinpour, A. Saeidi, M. Salsabili, M. Nastev, M.-J. Nollet, Development of a probabilistic seismic microzonation software considering geological and geotechnical uncertainties, Georisk 1-21. https://doi.org/10.1080/17499518.2024.2302183.
[50] M. Salsabili, A. Saeidi, A. Rouleau, M. Nastev, Development of empirical CPTu-Vs correlations for post-glacial sediments in Southern Quebec, Canada, in consideration of soil type and geological setting, Soil Dynam. Earthq. Eng. 154 (2022) 107131, https://doi.org/10.1016/j.soildyn.2021.107131.
[51] G. Toro, Probabilistic Models of Site Velocity Profiles for Generic and Site-specific Ground-Motion Amplification Studies, Technical Rep 779574, 1995.
[52] E.M. Rathje, A.R. Kottke, W.L. Trent, Influence of input motion and site property variabilities on seismic site response analysis, J. Geotech. Geoenviron. Eng. 136 (4) (2010) 607–619. https://10.1061/(ASCE)GT.1943-5606.0000255.
[53] S.L. Kramer, Geotechnical Earthquake Engineering, Prentice Hall, 1996.
[54] E. Azzouz, Recherche sur la vulnérabilité sismique des équipements électriques au Québec, Rapport, UQAC, 2021.
[55] H. Pan, L. Tian, X. Fu, H. Li, Sensitivities of the seismic response and fragility estimate of a transmission tower to structural and ground motion uncertainties, J. Constructional Steel Res. 167 (2020) 105941.
[56] FEMA, Hazus-MH 2.1 Technical Manual, FEMA Washington, DC, 2012.
[57] M. Kolaj, J. Adams, S. Halchuk, The 6th generation seismic hazard model of Canada. 17th World Conference on Earthquake Engineering, Sendai, Japan, 2020. Paper 1c-0028.